Synthesis of Bessel Beam Using Time-Reversal Method Incorporating Metasurface

QING-SONG JIA[1], **SHUAI DING**[1], **HUI-BING DONG**[1], **XU HAN**[1], **ZHAO-JUN ZHU**[1],
BING-ZHONG WANG[1], **(Senior Member, IEEE), YONG MAO HUANG**[1,2], **(Member, IEEE),**
AND MAURIZIO BOZZI[3], **(Fellow, IEEE)**

[1]Institute of Applied Physics, University of Electronic Science and Technology of China, Chengdu 610054, China
[2]School of Electrical and Electronic Engineering, Xihua University, Chengdu 610039, China
[3]Department of Electrical, Computer and Biomedical Engineering, University of Pavia, 27100 Pavia, Italy

Corresponding authors: Shuai Ding (uestcding@uestc.edu.cn) and Yong Mao Huang (ymhuang1988@126.com)

ABSTRACT In this paper, a synthesis and implementation method for generating Bessel beams based on time-reversal theory incorporating electromagnetic (EM) meta-lens is proposed. As is known, time-reversal EM waves has the unique characteristic of adaptive backtracking. Therefore, with this characteristic, the EM characteristics of the radiation aperture can be obtained and further utilized to generate Bessel waves with any departure angle. Based on this concept, two meta-lenses for generating Bessel beams tilted in different directions were designed. Both meta-lenses were designed at the center frequency of 15 GHz, and the simulation results were consistent with the target expectation. A representative meta-lens was fabricated and measured. The final size of the meta-lens was 350 mm × 350 mm, and a Bessel beam with a 30° emergence angle was generated by this structure. The experimental results were in good agreement with the simulation results and the theoretical derivation. This synthetic method of Bessel beam generation using the time-reversal operation may be of great use for the application of Bessel beams in microwave communications, and it can broaden the application scope of non-diffracting beams.

INDEX TERMS Arbitrary direction tilted Bessel beam, time-reversal, high transmissivity, transmissive metasurface.

I. INTRODUCTION

Diffraction is one of the basic physical phenomena of electromagnetic (EM) wave propagation. Bessel beam is a kind of non-diffracting wave (NDW) that can retain a certain shape in space [1], [2]. EM waves diffuse in all directions of space in the process of propagation, which leads to the decline of the receiving efficiency and the spatial resolution. However, Bessel beams have high directionality and are non-diffracting [3]. They will be widely used in the fields of dense channel communication, high-resolution microwave imaging [4], [5], efficient wireless energy transmission, and other application scenarios [6]–[10].

As a new EM wave control method, use of an artificial EM metasurface can flexibly control the amplitude, phase, and

The associate editor coordinating the review of this manuscript and approving it for publication was Bilal Khawaja.

polarization of an EM wave [11], [12]. With the advantages described above, the meta-lens is more convenient for the synthesis of various beams [13], [14]. In this paper, we use the transmissive metasurface as a lens to control the Bessel beam.

An innovation of this paper is that time-reversal (TR) electromagnetism is integrated with Bessel beam formation. This efficient method of generating Bessel beams is proposed and verified in this paper. TR electromagnetism is a new research field [15]. Due to the symmetry of the Maxwell equations, TR electromagnetic wave propagation in an ideal TR cavity has the characteristic of perfect backtracking [16]–[20], which will be of great use for the generation of Bessel beams.

In previous studies, many Bessel-beam-generating devices have been proven to be feasible for the synthesis of various Bessel beams [21], [22]. However, low efficiency and large size are common in these devices [23]–[26], and the reflective

metasurface always has the problem of limited usage scenarios [27]. Furthermore, most Bessel beam generation methods only focus on how to generate a Bessel beam perpendicular to the transmitting surface [28], [29], which places large restrictions on the transmission of Bessel beams, and the use scenario is relatively simple because the transmitting and receiving positions must be vertically aligned. To solve this problem, we designed a lens that can produce Bessel beams with any inclination angle using the TR method. At the same time, the lens can convert plane waves into Bessel beams that propagate in the specified direction [20].

II. PRINCIPLE

As early as 1941, Stratton presented the non-diffracting solution of the wave equation in his works [30]. This kind of solution shows that the cross-section field of an EM wave is a Bessel function distribution during the propagation process, and the beam does not diffract with the increase in distance. In 1987, *Durnin et al.* proved that Bessel beams can be generated using finite devices, which makes the research of Bessel beams more and more attractive [31]. In this section, based on TR electromagnetism, an efficient method of generating Bessel beams is proposed. The method was verified by simulations.

A. BESSEL BEAM THEORY

In the cylindrical coordinate system, the scalar wave equation is solved by the method of separation of variables [32]. The form of the solution of the electric field is $E = R(r)\Phi(\varphi)Z(z)$. The solution can be readily obtained in the z and φ-directions. Including the dependence on time t, the form of the solution of the electric field is obtained as follows:

$$E = R(r)\exp(ik_z z + im\varphi - i\omega t). \qquad (1)$$

After separating variables, the radial differential equation is as follows:

$$r^2\frac{d^2R}{dr^2} + r\frac{dR}{dr} + [(k^2 - k_z^2)r^2 - m^2]R = 0, \qquad (2)$$

where $k^2 = k_r^2 + k_z^2$. Equation (2) is the Bessel differential equation. Generally, the solutions of the Bessel equation are two functions, namely, the Bessel function of the first kind $J_m(k_r r)$ and the Bessel function of the second kind $N_m(k_r r)$. However, in free space, the EM waves radiated from the point source need to satisfy the boundary conditions; that is, there is no field source at infinity in the free space, expressed as follows:

$$\lim_{r\to\infty} r^{\frac{1}{2}}(\frac{dR}{dr} - ik_r R) = 0. \qquad (3)$$

The Bessel functions of the first and second kind do not satisfy this condition, but the Hankel function does. It is a linearly independent solution of the Bessel differential equation and can be regarded as a linear combination of the Bessel functions of the first and second kind. The Hankel functions are expressed as follows:

$$H_m^1(k_r r) = J_m(k_r r) + iN_m(k_r r)$$

$$H_m^2(k_r r) = J_m(k_r r) - iN_m(k_r r). \qquad (4)$$

It can be concluded that the solutions of the wave equation in the cylindrical coordinate system in free space are:

$$\begin{aligned}E^1(r, \varphi, z, t)\\= [J_m(k_r r) + iN_m(k_r r)]\exp(ik_z z + im\varphi - i\omega t)\\E^2(r, \varphi, z, t)\\= [J_m(k_r r) - iN_m(k_r r)]\exp(ik_z z + im\varphi - i\omega t). \quad (5)\end{aligned}$$

E^1 and E^2 represent the EM waves propagating inward and outward along the Z-axis, respectively, and the internal traveling wave will become the external traveling wave along the Z-axis. Therefore, the electric field distribution on the Z-plane can be regarded as the linear superposition of E^1 and E^2, and the electric field amplitude is:

$$E(r, \varphi, z, t) = 2J_m(k_r r)\exp(ik_z z + im\varphi - i\omega t), \qquad (6)$$

where m represents the order of the Bessel function. When $m = 0$, the solution of Equation (6) is the solution of the zero-order Bessel function, i.e., the Bessel beam in the traditional sense.

B. TIME-REVERSAL BESSEL BEAM SYNTHESIS METHOD

In contrast to the traditional method of Bessel beam synthesis, TR synthesis of Bessel beams does not directly synthesize the electric field distribution of the Bessel beam but uses the TR method to synthesize a pre-distorted Bessel beam electric field distribution [33]. Due to the TR electromagnetic wave has the adaptive backtracking characteristic, if its electric field distribution satisfies the electric field distribution of the Bessel beam when it propagates to the specified position, the TR electromagnetic wave will continue to propagate in the form of a Bessel beam. In the isotropic passive position, the EM field ($\mathbf{E}$, $\mathbf{H}$) in the region satisfies the homogeneous vector wave equation [34], [35]:

$$\nabla^2\mathbf{E}(\boldsymbol{r}, t) - \mu\varepsilon\frac{\partial^2}{\partial t^2}\mathbf{E}(\boldsymbol{r}, t) = 0$$

$$\nabla^2\mathbf{H}(\boldsymbol{r}, t) - \mu\varepsilon\frac{\partial^2}{\partial t^2}\mathbf{H}(\boldsymbol{r}, t) = 0, \qquad (7)$$

$\mathbf{E}(\boldsymbol{r}, t)$ as another solution of the vector wave equation can be obtained by TR operation. After mathematical treatment on the left side, Equation (7) could be expressed as follows:

$$\begin{aligned}&\nabla^2\mathbf{E}(\boldsymbol{r}, -t) - \mu\varepsilon\frac{\partial^2}{\partial t^2}\mathbf{E}(\boldsymbol{r}, -t)\\&= \nabla^2\mathbf{E}(\boldsymbol{r}, \tau) - \mu\varepsilon\frac{\partial^2}{\partial(-\tau)^2}\mathbf{E}(\boldsymbol{r}, \tau)\\&= \nabla^2\mathbf{E}(\boldsymbol{r}, \tau) - \mu\varepsilon\frac{\partial^2}{\partial(\tau)^2}\mathbf{E}(\boldsymbol{r}, \tau) = 0. \quad (8)\end{aligned}$$

For the frequency domain, we assume that a time domain signal is u, and its Fourier transform expression is

$$U(\boldsymbol{r}, \omega) = \int u(\boldsymbol{r}, t)e^{-j\omega t}dt. \qquad (9)$$

Because u is a real signal, so $U(\mathbf{r}, -\omega) = U^*(\mathbf{r}, \omega)$, U^* is expressed as conjugate, so for the TR signal of u, we can get:

$$U^{TR}(\mathbf{r}, \omega) = \int u(\mathbf{r}, -t)e^{-j\omega t} dt$$

$$= \int u(\mathbf{r}, \tau)e^{-j(-\omega)\tau} d\tau$$

$$= U(\mathbf{r}, -\omega) = U^*(\mathbf{r}, \omega). \qquad (10)$$

$U^{TR}(\mathbf{r}, \omega)$ is the frequency domain form corresponding to the TR signal. We can see that the TR operation is equivalent to the phase conjugation operation at each frequency point. The detailed processes of generating a Bessel beam by TR was as following:

First of all, the numerical model of the Bessel beam to be generated was established, the frequency of the Bessel beam was determined, and the electric and magnetic field distributions were obtained, which were used as the incident wave source. By means of a numerical simulation, we then established a Bessel beam propagation field in a certain position in space.

Secondly, the Bessel beam was simulated and launched by a finite aperture, and its propagation in free space was analyzed and observed. A finite aperture time-reversal mirror (TRM) was used to collect the incident information. For the Bessel beam with a single frequency, the information was mainly the electric field information, and the information obtained using the TRM was mainly the information of its electric and magnetic field components. Therefore, the phase conjugation operation could be carried out using the information at each position.

Finally, according to the collected incident wave information, the TR operation was carried out, and the TRM was used to transmit it again to simulate the backtracking of the TR electromagnetic wave and the reconstruction characteristics of the dynamic non-diffracting EM wave. Because of its characteristics of backtracking, ideally, the pre-distorted EM wave will be continuously traced back to the emission source in the process of propagation and form the same electric field distribution as that of the emission source when it reaches the original emission position. After this, it will continue to propagate for a certain distance with slight diffraction.

In the proposed method, the TRM plays three roles [36], [37]: (1) collecting the incident Bessel beam information, (2) realizing the TR operation of the collected electric field information, and (3) transmitting the inverse field.

The first two functions can be simulated in the numerical model, but the last function needs the actual device to control the electric field. Because the meta-lens has an excellent regulation effect on the electromagnetic wave, we chose to use the meta-lens to realize the emission function of the TRM.

III. DESIGN OF META-LENS
In this section, we design the meta-lens which a plane wave passing through will transform a Bessel beam. To ensure the high efficiency of the beam, we design an efficient cell that the phase can be adjusted in the range of 0°–360°. Using
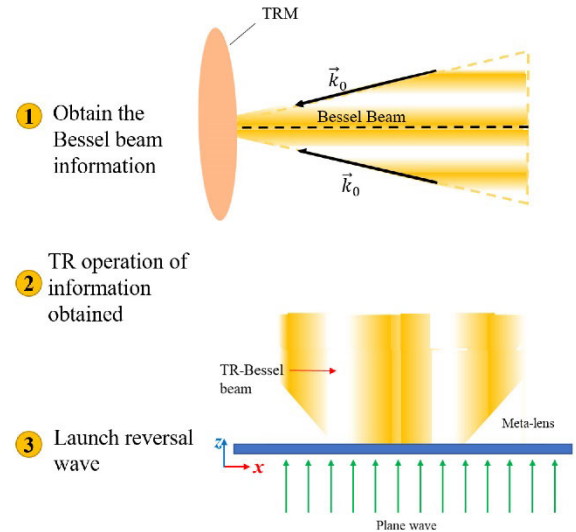

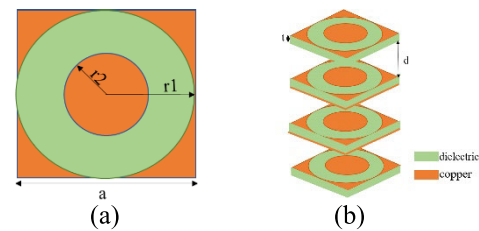**FIGURE 1.** Schematic diagram of generation process of TR Bessel beam.

FIGURE 2. Meta-lens unit structure diagram: (a) front view of unit cell structure and (b) perspective of meta-lens unit cell structure.

the cells, two kinds of meta-lens generating Bessel beam are designed.

A. DESIGN OF ELECTROMAGNETIC META-LENS CELL
To avoid the large phase shift error caused by machining deflection errors, the cell must exhibit a good transmission performance. At the same time, the phase range of this cell should be greater than or equal to 360°, and the change of phase shift curve should be optimal. In this work, a multilayer meta-lens element structure is designed. As shown in Fig. 2, the unit period was 7 mm, the working frequency was 15 GHz, the thickness of the dielectric substrate was $t = 0.8$ mm, the dielectric constant was $\varepsilon_r = 2.65$, the outer diameter of the annular hole was $r1 = 3.5$ mm, the interval between layers was $d = 4.2$ mm, and the thickness of metal layer was 0.035 mm. To increase the transmission and phase control range, a four-layer plate structure was used, and the distance between the two plates was 4.2 mm. The meta-lens cell had double-layer metal middle patches, and single-layer metal top and bottom patches.

B. DESIGN OF VERTICAL BESSEL BEAM LENS
In the previous section, we designed a metasurface unit cell with a high transmittance and adjustable 360° range. To convert a plane wave into a TR Bessel beam, the most important thing is to determine the phase change of each position in the plane.
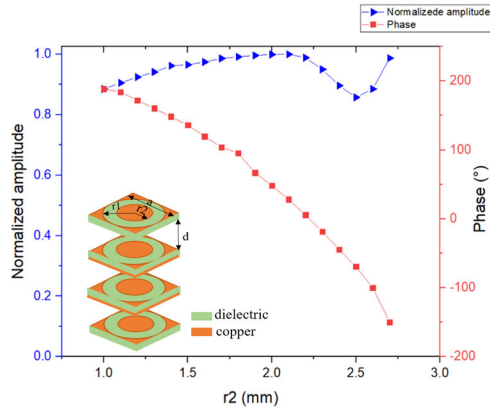
FIGURE 3. Relationship between element inner diameter r2 and transmission phase and amplitude.

FIGURE 4. Simulation diagram of standard Bessel wave and the electric field distribution of this Bessel beam source.

To obtain the phase shift of each position, a Bessel beam was simulated for emission, and the electric field distribution of its cross-section was obtained during its propagation process. The electric field information was then extracted by numerical calculation to obtain the phase distribution, and then the phase conjugation operation was carried out. Because the period length was a, it was necessary to determine the phase change at $(x \cdot a, y \cdot a)$ based on the phase conjugation of the electric field obtained by numerical calculation to determine the unit structure size at this position. Finally, the plane wave was applied to the meta-lens. After adjusting the plane wave at each position of the meta-lens, the phase of the whole outgoing electric field was consistent with the TR Bessel beam to be synthesized.

The parameters of the Bessel beam in the full-wave simulation software (CST STUDIO SUITE) were consistent with those described above. The frequency was 15 GHz, the radial wave number was $k_x = k_\rho = (-0.4 - i0.02)k_0$, the radius of the wave source was 100 mm, the polarization direction was linear in the X-direction, and the expression of the electric field was

$$\begin{cases} E_x(r, \phi, z) = \exp(ik_z z)J_0(k_x r) \\ E_y(r, \phi, z) = 0 \\ E_z(r, \phi, z) = 0 \end{cases} \tag{11}$$

The electric field information was imported into the full-wave simulation. An electric field monitor was set up in the software, and an electric field observation surface was set up 150 mm from the emission surface to record the electric field information. Simulation diagram of Bessel beam, and the electric field distribution of this Bessel beam source are shown in Fig. 4.

The size of the observation surface was 350 mm $\times$ 350 mm. Since this observation plane was equivalent to the TRM of the TR operation, it needed to be larger than the whole Bessel source to ensure the integrity of the information.

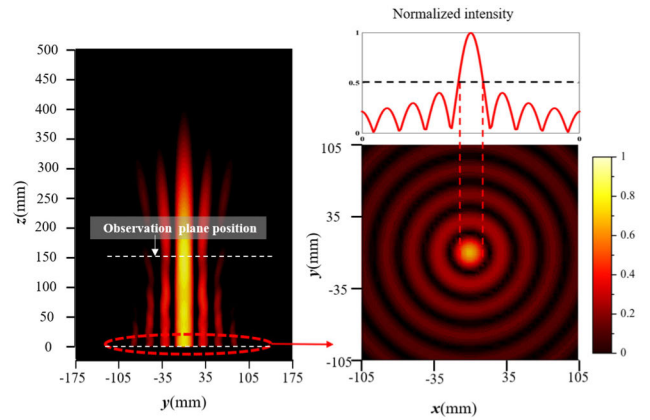Since the electric field component had only an Ex component, only the phase and amplitude information of the Ex field

was needed to extract the phase distribution of the electric field. A phase conjugation operation was then conducted on the extracted electric field information, and the phase information obtained was the compensation phase value required by each meta-lens unit. The phase compensation values of each position are shown in Figs. 5 (a).

The observation plane was the receiving function of the detector instead of the TRM array, and the meta-lens was used to replace the transmitting function of the TRM array. To ensure consistency, the size of the meta-lens and the observation surface was 350 mm $\times$ 350 mm, and there were 50 element structures along the X- and Y-directions.

According to the corresponding relationship between the size of the element structure and the transmission phase change, the element size distributions at different positions of the meta-lens were determined. Due to the large number of cells in the whole meta-lens, up to 2500 units, numerical simulation was used to call the interface in the full-wave simulation software, to map the distribution and the unit structure size, and to establish the topological structure of the whole meta-lens, as shown in Figs. 5 (b). This approach improved the modeling efficiency.

C. DESIGN OF TILTED BESSEL BEAM META-LENS

As the conventional method is used to synthesize the Bessel beam, the analytic expression of the Bessel beam should be provided, and the field synthesis should be carried out. However, it is difficult to synthesize the surface directly because of the complexity of the traditional method. In this section, the TR method is still used to comprehensively design the metasurface. The whole generation process of the tilted Bessel beam is shown in Fig. 6.

Firstly, since it is difficult to directly simulate the emission source of the inclined Bessel beam, we established an inclined electric field observation surface in the propagation range of the zero-order Bessel beam and determined the tilt angle $\theta = 30°$. The phase conjugation operation was carried out to record the electric field information of the inclined plane, and the phase distribution characteristics of each element of the
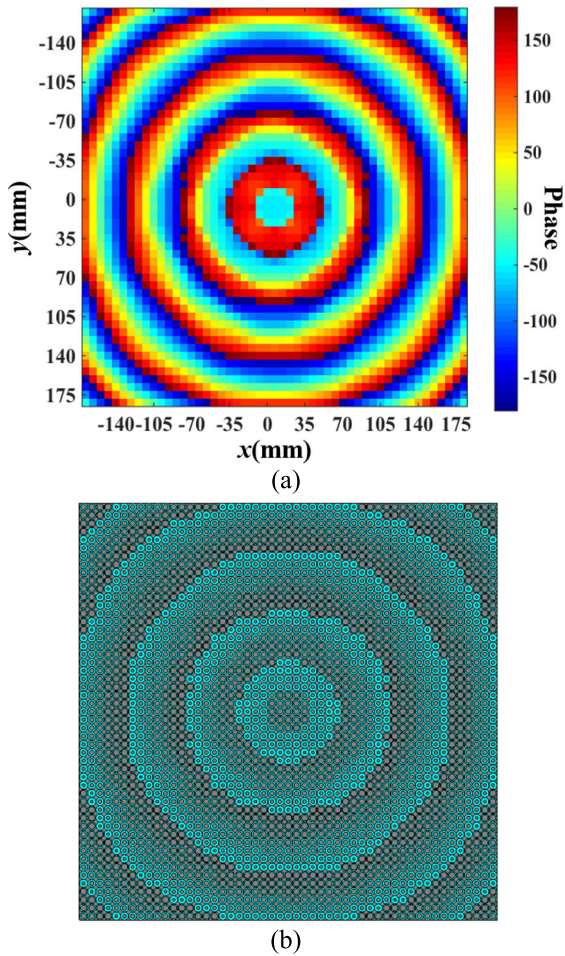
FIGURE 5. (a) Phase distribution of TR Bessel beam and (b) TR Bessel lens structure.

FIGURE 7. (a) Phase distribution of the designed tilted TR Bessel beam and (b) structure of tilted Bessel beam lens.
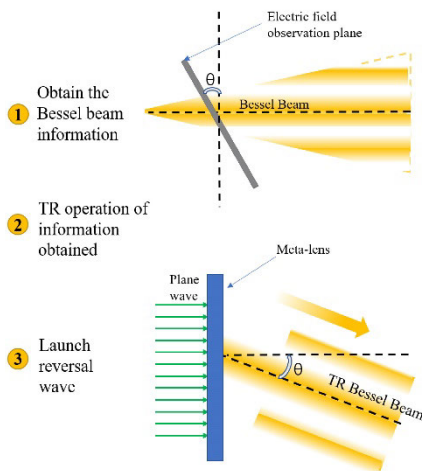

FIGURE 6. Schematic diagram of tilted Bessel beam generation process.

whole meta-lens were obtained by discrete sampling of the recorded electric field information, which was equivalent to receiving the inclined Bessel beam directly using the vertical observation plane. The TR Bessel beam with a specific tilt
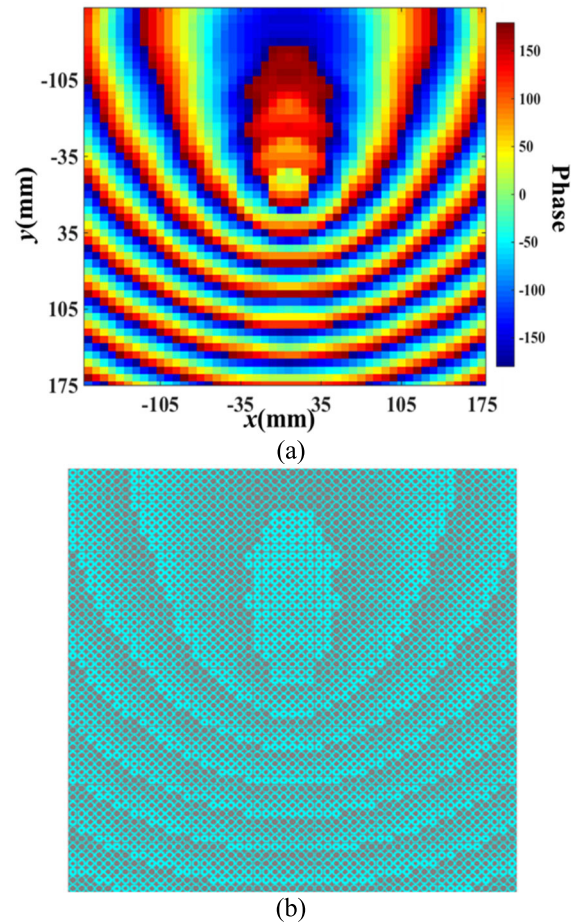
angle was obtained by irradiating the meta-lens with a plane wave.

The size of the established meta-lens was consistent with the observation surface and contained 50 units along the X- and Y-directions. The relative dielectric constant of the dielectric substrate was $\varepsilon_r = 2.65$. The phase distribution of the central position of each unit is shown in Fig. 7(a).

Using the designed high-efficiency transmission structure, we can obtain the unit structure parameters at different positions by the one-to-one correspondence between the center positions of the surface and the element size structure. The structure of the tilted Bessel beam lens is shown in Figs. 7(b).

IV. RESULTS AND DISCUSSIONS

In the previous section, we designed a transmission-type phase control unit with a high transmittance and a vertical and inclined meta-lens using the TR method. In this section, we present the simulation results and analysis of the two kinds of meta-lenses using the full-wave simulation. We measured the tilted Bessel beam meta-lens in the microwave anechoic chamber to analyze whether it was consistent with the simulation results. Finally, the feasibility of this method was verified.

A. SIMULATIONS AND OPTIMIZATIONS

B. 1)VERTICAL BESSEL BEAM LENS

The established meta-lens was simulated in the full-wave

simulation software. A plane wave was used to irradiate the meta-lens, and the electric field monitors were set up on the *YOZ* and *XOZ* planes to observe the beam propagation characteristics of the longitudinal field. At the same time, the monitors were set up at three different positions of $z = 100$, 200, and 300 mm to comprehensively analyze the energy distribution of the whole Bessel beam propagation process.

Figs. 8 (a) shows the electric field intensity distribution in the propagation direction of the plane wave after passing through the meta-lens. The whole beam was a completely symmetric EM wave, and the beam energy did not diffuse in a certain area with the increase in the propagation distance during the propagation process. Figs. 8 (b) shows the distribution of the electric field intensity in the *XOY* plane at $z = 100$ mm. When the position of the electric field detector was 150 mm from the source of the Bessel beam, the whole TR beam did not trace back to the Bessel beam shape and was still in a predistortion state. Figs. 8 (c) represents the distribution of the *XOY* plane electric field intensity at $z = 200$ mm. The beam center energy was significantly enhanced compared with that in Figs. 8 (b), and the whole field energy corresponded to a circular Bessel beam. Figs. 8 (d) shows the *XOY* energy distribution at $z = 300$ mm, and the energy intensity was not significantly reduced compared with that in Figs. 8 (c). From another point of view, it was proven that the TR Bessel beam obtained from the meta-lens had non-diffracting characteristics.

The comparison of the above simulation results showed that the TR Bessel beam had the characteristic of predistortion, and it did not show the Bessel beam characteristics initially. However, it showed the Bessel beam characteristics after reaching a certain distance, which is consistent with our analysis in Section II. The meta-lens introduced in this section can convert a plane wave into a kind of TR Bessel beam that we specify. We call such a meta-lens structure the TR Bessel beam lens. The whole meta-lens functions as a TRM to transmit TR information. This section also proves the feasibility and correctness of the TR Bessel beam synthesis.

C. TILTED BESSEL BEAM LENS

The model of the tilted Bessel beam lens was established in the full-wave simulation. The simulation results showed that the meta-lens could generate a TR Bessel beam with an inclination angle of 30°. The electric field monitor was placed in the cross section of three different positions in the propagation direction to observe the amplitude information of the electric field component.

An electric field monitor was set up in the vertical direction (*YOZ* plane) to provide the electric field information in the propagation direction and to judge the beam propagation characteristics. Using the conditions described above,
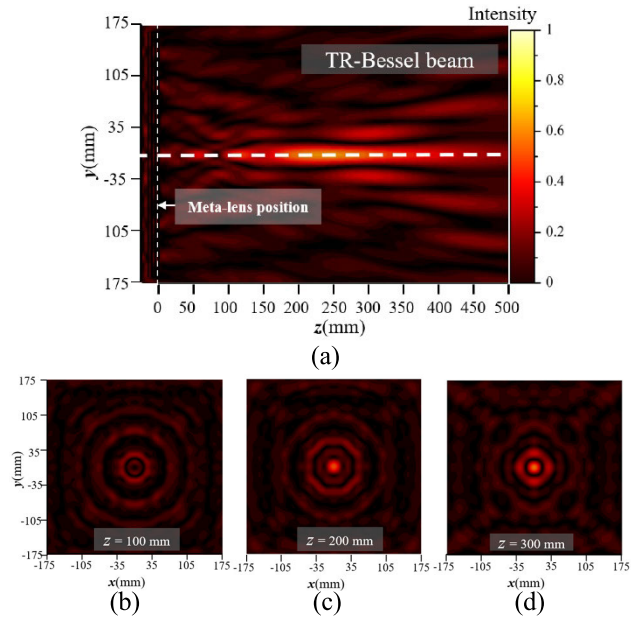

FIGURE 8. Electric field intensity distribution diagram of the transmission wave of the vertical Bessel lens. (a) Energy distribution of the seeding field on the YOZ plane. Energy distributions of the cross sections (b) 100 mm, (c) 200 mm, and (d) 300 mm from the transmission Bessel meta-lens.

a simulation was conducted in the full-wave simulation software, and the transmission electric field amplitude distribution through the meta-lens was obtained, as shown in Figs. 9. Figs. 9 (a) shows the electric field intensity distribution in the propagation direction of the plane wave after passing through the meta-lens. The whole beam propagated with an inclination angle of 30°, and the electric field intensity remained constant until 400 mm during the whole propagation process without attenuation. Figs. 9 (b) shows that the energies of the main beam and the annular side lobe of the whole field were weak, and the information of the whole propagation field was not reconstructed. Figs. 9 (c) represents the distribution of the *XOY* plane electric field intensity at $z = 200$ mm, and the beam center energy was significantly enhanced compared with that shown in Figs. 9 (b). Figs. 9 (d) shows the XOY energy distribution at z = 300 mm, which shows that the energy did not decrease significantly.

D. MEASUREMENT RESULTS AND DISCUSSION

The tilted Bessel beam lens designed in this paper was physically fabricated. The dielectric constant of the dielectric base plate was $\varepsilon_r = 2.65$, which was consistent with the simulation. The thickness of the metal structure was 0.035 mm, the thickness of the dielectric was 0.8 mm, the size of the dielectric was 400 mm × 400 mm, and the meta-lens structure was 350 mm × 350 mm. The redundant component was used to fix and assemble the four dielectric substrates, and each dielectric substrate was separated by a 4.2-mm-high air layer in the middle using a dielectric nut spacer, consistent with the unit structure. The physical drawing of the process is shown in Figs. 10(a).
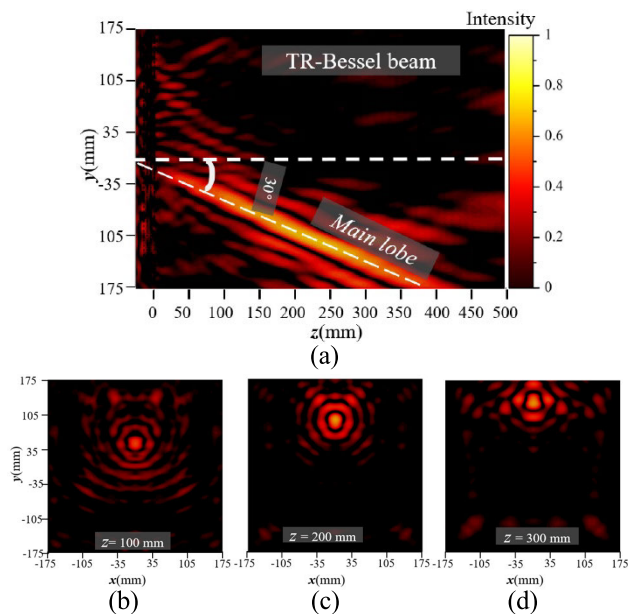
(a)

(b)   (c)   (d)

FIGURE 9. Electric field intensity distribution diagram of tilted Bessel lens: (a) normalized intensity distribution of electric field in YOZ plane when x = 0 mm. Electric field intensity distribution of transverse section when (b) z = 100 mm, (c) z = 200 mm, and (d) z = 300 mm.

The fabricated meta-lens was put into the microwave ane-choic chamber for measurement. A plane wave conversion lens was used to convert the spherical wave emitted by the antenna into a plane wave. The distance between the transmit-ting antenna and the plane wave conversion lens was 375 mm, and the distance between the plane lens and the meta-lens was 50 mm. The whole field scanning ranges were 600 mm along the Z-axis and 380 mm along the X- and Y-axes, with a scanning interval of 2 mm. The experimental setup is shown in Figs. 10(b) and 10(c).

In the experiment, the near-field normalized electric field amplitude distribution of the YOZ plane at $x = 0$ mm at the working frequency of 15 GHz was scanned and recorded. The results are shown in Fig. 11. To observe the experimental results more intuitively, we added auxiliary lines to the main beam. The whole TR Bessel beam radiated outward in an inclined state of $30°$. The energy of the whole beam was concentrated on the main beam, and the energy had not diffused during the propagation process. The main beam had a large energy before $x = 400$ mm.

The XOY planes at $z = 100$, 200, 300, and 400 mm were scanned and measured in this experiment. The normalized electric field distribution in the plane is shown in Fig. 12. The energy distribution of the beam was not evident, in contrast to the simulation results, but the energy of the plane beam was concentrated at one point. This proved that the non-diffracting characteristics of the beam were good, and the beam shape did not spread until 400 mm.

Compared with the simulation, the measured non-diffracting distance was smaller than that in the simulation case. This was because the inaccuracy of machining and measurement, and another important reason was that the lens
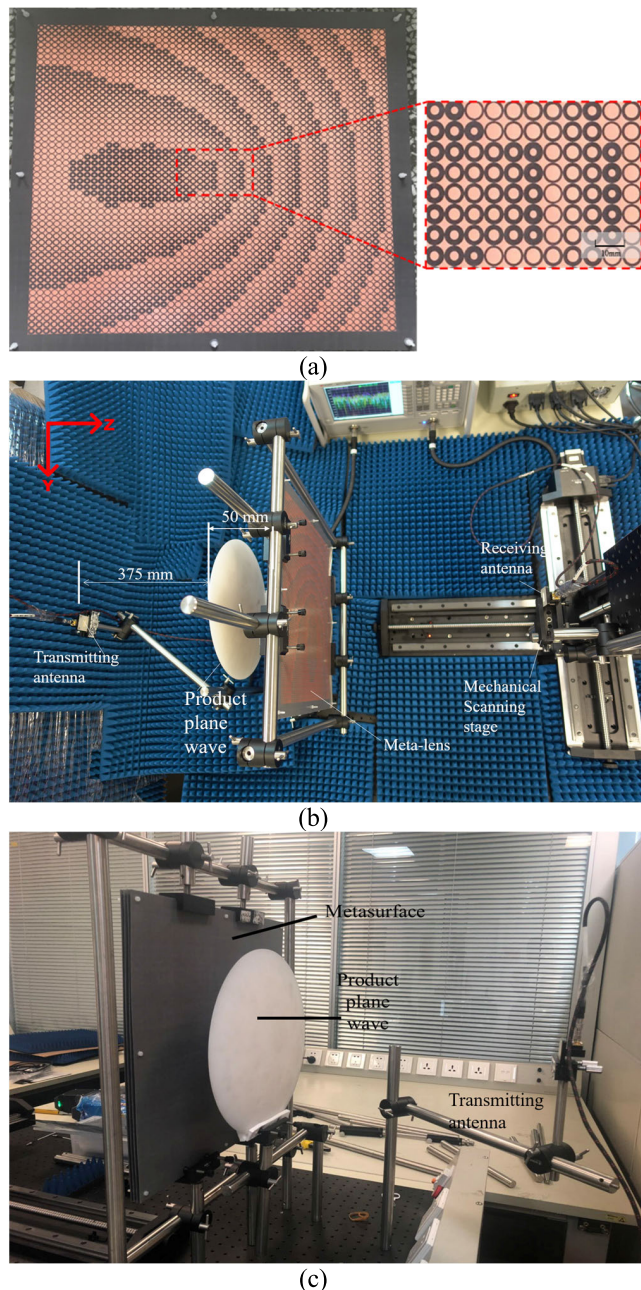

(a)

(b)

(c)

FIGURE 10. (a) Prototype of the fabricated tilted Bessel beam lens. (b) and (c) Experimental system configuration for the fabricated tilted Bessel beam lens.

producing the plane wave was smaller than our TR tilted Bessel beam lens, which led to a phase difference between the electric field at the edge and the ideal TR electric field, and the effective aperture of the whole TR lens decreased compared with that of the ideal case. The ring energy distributions of the measured electric field on the four XOY surfaces were uneven. The reason for the uneven distribution may have been that the energy of the annular field was not significant due to the small side lobe energy of the beam itself and some scattering in the space. The main energy was concentrated on the central main beam, and the whole sampling interval
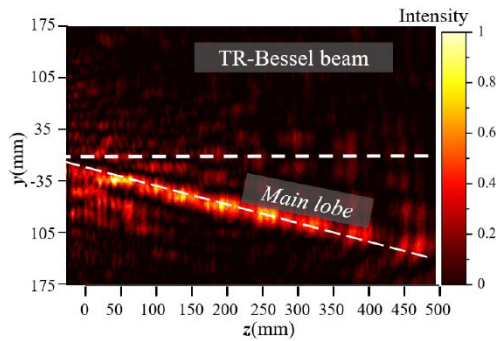
FIGURE 11. Normalized diagram of electric field amplitude distribution on YOZ surface.
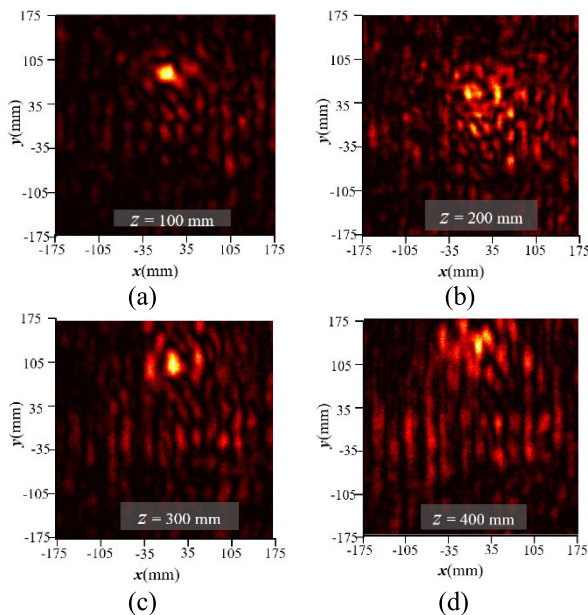

FIGURE 12. XOY plane electric field amplitude distributions of electric field intensity at (a) z = 100 mm, (b) z = 200 mm, (c) z = 300 mm, and (d) z = 400 mm.

was larger than the simulation interval. Consequently, the ring distribution not evident.

According to Fig. 11 and Figs.12, it can be concluded that the measured results of the whole TR tilted Bessel beam lens were basically consistent with the simulation results. This lens can transform plane waves into tilted non-diffracting waves, which gives the Bessel beam good directivity and broadens its application scope.

V. CONCLUSION

In this paper, based on a transmission-type phase control unit with a high transmittance, two kinds of meta-lenses were designed to generate different forms of zero-order Bessel beams using the TR method. The unit can adjust and control the phase in the range of 0°–360°, and the phase regulation relationship changes linearly with the size change. In contrast to the traditional method, which directly uses the optical convergence formula, we obtain the phase distribution of the meta-lens through the TR method. We use this meta-lens to replace the transmitting function of the TRM to synthesize the

TR beam and obtain a whole meta-lens with a size of 350 mm × 350 mm, which can produce a vertical TR Bessel beam.

Based on these results, a meta-lens that can generate inclined Bessel beams was designed. At present, there have been few studies on the method of producing titled Bessel beams. The electric field amplitude at different positions was measured by near-field scanning in a microwave anechoic chamber, and the inclined Bessel beam could be generated on the meta-lens.

The experimental results showed that this method is feasible and efficient. Different angles of the zero-order Bessel beams were generated successfully using meta-lenses, which broadens the application scope of Bessel beams in the microwave field. Furthermore, the TR method also simplifies the synthesis difficulty of different shapes of the Bessel beams.

REFERENCES

[1] J. Durnin, J. J. Miceli, and J. H. Eberly, "Diffraction-free beams," *Phys. Rev. Lett.*, vol. 58, pp. 1499–1501, Apr. 1987.

[2] Z. Bouchal and M. Olivík, "Non-diffractive vector Bessel beams," *Optica Acta Int. J. Opt.*, vol. 42, no. 8, pp. 1555–1566, 1995.

[3] S. Xu, Y. Li, X. Liang, H. Cao, M. Hu, L. Chai, and C. Wang, "Generation of terahertz radiation by optical rectification using femtosecond Bessel beam," *IEEE J. Sel. Topics Quantum Electron.*, vol. 23, no. 4, pp. 1–6, Jul. 2017.

[4] M. Cheng, L. Guo, J. Li, and Y. Zhang, "Channel capacity of the OAM-based free-space optical communication links with Bessel–Gauss beams in turbulent ocean," *IEEE Photon. J.*, vol. 8, no. 1, pp. 1–11, Feb. 2016.

[5] X. Wang, D. R. Bauer, R. Witte, and H. Xin, "Microwave-induced thermoacoustic imaging model for potential breast cancer detection," *IEEE Trans. Biomed. Eng.*, vol. 59, no. 10, pp. 2782–2791, Oct. 2012.

[6] X. Wang, D. R. Bauer, J. L. Vollin, D. G. Manzi, R. S. Witte, and H. Xin, "Impact of microwave pulses on thermoacoustic imaging applications," *IEEE Antennas Wireless Propag. Lett.*, vol. 11, pp. 1634–1637, 2012.

[7] L. Niu, K. Wang, Y. Yang, Q. Wu, X. Ye, Z. Yang, J. Liu, and H. Yu, "Diffractive elements for zero-order Bessel beam generation with application in the terahertz reflection imaging," *IEEE Photon. J.*, vol. 11, no. 1, pp. 1–12, Feb. 2019.

[8] D. Mcgloin, V. Garcés-Chávez, and K. Dholakia, "Interfering Bessel beams for optical micromanipulation," *Opt. Lett.*, vol. 28, no. 8, pp. 657–659, 2003.

[9] B. Hafizi, E. Esarey, and P. Sprangle, "Laser-driven acceleration with Bessel beams," *Phys. Rev. E, Stat. Phys. Plasmas Fluids Relat. Interdiscip. Top.*, vol. 55, no. 3, pp. 3539–3545, Mar. 1997.

[10] M. K. Bhuyan, F. Courvoisier, P. A. Lacourt, M. Jacquot, R. Salut, L. Furfaro, and J. M. Dudley, "High aspect ratio nanochannel machining using single shot femtosecond Bessel beams," *Appl. Phys. Lett.*, vol. 97, no. 8, p. 219, 2010.

[11] N. Yu, F. Capasso, Z. Gaburro, J.-P. Tetienne, P. Genevet, F. Aieta, M. A. Kats, R. Blanchard, and G. Aoust, "Flat optics: Controlling wavefronts with optical antenna metasurfaces," *IEEE J. Sel. Topics Quantum Electron.*, vol. 19, no. 3, May/Jun. 2013, Art. no. 4700423.

[12] J. Wen, L. Chen, B. Yu, J. B. Nieder, S. Zhuang, D. Zhang, and D. Lei, "All-dielectric synthetic-phase metasurfaces generating practical airy beams," *ACS Nano*, vol. 15, no. 1, pp. 1030–1038, Jan. 2021.

[13] J. Fan, Y. Cheng, and B. He, "High-efficiency ultrathin terahertz geometric metasurface for full-space wavefront manipulation at two frequencies," *J. Phys. D, Appl. Phys.*, vol. 54, no. 11, Mar. 2021, Art. no. 115101.

[14] F. Aieta, P. Genevet, M. A. Kats, N. Yu, R. Blanchard, Z. Gaburro, and F. Capasso, "Aberration-free ultrathin flat lenses and axicons at telecom wavelengths based on plasmonic metasurfaces," *Nano Lett.*, vol. 12, no. 9, pp. 4932–4936, 2012.

[15] G. Lerosey, J. D. Rosny, A. Tourin, A. Derode, G. Montaldo, and M. Fink, "Time reversal of electromagnetic waves and telecommunication," *Radio Sci.*, vol. 40, no. 6, pp. 1–10, Dec. 2005.

[16] Y. Chen and B. Z. Wang, "Polycentric spatial focus of time-reversal electromagnetic field in rectangular conductor cavity," *Opt. Exp.*, vol. 21, no. 22, pp. 26657–26662, 2013.

[17] G. F. Edelmann, T. Akal, W. S. Hodgkiss, S. Kim, W. A. Kuperman, and H. C. Song, "An initial demonstration of underwater acoustic communication using time reversal," *IEEE J. Ocean. Eng.*, vol. 27, no. 3, pp. 602–609, Jul. 2002.

[18] K. Wang, W. Shao, H. Ou, and B.-Z. Wang, "Time-reversal focusing beyond the diffraction limit using near-field auxiliary sources," *IEEE Antennas Wireless Propag. Lett.*, vol. 16, pp. 2828–2831, 2017.

[19] D. Zhao, Y. Jin, B.-Z. Wang, and R. Zang, "Time reversal based broadband synthesis method for arbitrarily structured beam-steering arrays," *IEEE Trans. Antennas Propag.*, vol. 60, no. 1, pp. 164–173, Jan. 2012.

[20] G. Lerosey, J. D. Rosny, A. Tourin, and M. Fink, "Focusing beyond the diffraction limit with far-field time reversal," *Science*, vol. 315, no. 5815, pp. 1120–1122, Feb. 2007.

[21] M. Ettorre and A. Grbic, "Generation of propagating Bessel beams using leaky-wave modes: Experimental validation," *IEEE Trans. Antennas Propag.*, vol. 60, no. 8, pp. 3605–3613, Jun. 2012.

[22] B. G. Cai, Y. B. Li, W. X. Jiang, Q. Cheng, and T. J. Cui, "Generation of spatial Bessel beams using holographic metasurface," *Opt. Exp.*, vol. 23, no. 6, p. 7593, 2015.

[23] H. Zhang, X. Zhang, Q. Xu, C. Tian, Q. Wang, Y. Xu, Y. Li, J. Gu, Z. Tian, C. Ouyang, X. Zhang, C. Hu, J. Han, and W. Zhang, "High-efficiency dielectric metasurfaces for polarization-dependent terahertz wavefront manipulation," *Adv. Opt. Mater.*, vol. 6, no. 1, Jan. 2018, Art. no. 1700773.

[24] M. A. Salem, A. H. Kamel, and E. Niver, "Microwave Bessel beams generation using guided modes," *IEEE Trans. Antennas Propag.*, vol. 59, no. 6, pp. 2241–2247, Jun. 2011.

[25] A. Mazzinghi, M. Balma, D. Devona, G. Guarnieri, G. Mauriello, M. Albani, and A. Freni, "Large depth of field pseudo-Bessel beam generation with a RLSA antenna," *IEEE Trans. Antennas Propag.*, vol. 62, no. 8, pp. 3911–3919, Aug. 2014.

[26] S. Monk, J. Arlt, D. A. Robertson, J. Courtial, and M. J. Padgett, "The generation of Bessel beams at millimetre-wave frequencies by use of an axicon," *Opt. Commun.*, vol. 170, nos. 4–6, pp. 213–215, Nov. 1999.

[27] H. Liu, H. Xue, Y. Liu, Q. Feng, and L. Li, "Generation of high-order Bessel orbital angular momentum vortex beam using a single-layer reflective metasurface," *IEEE Access*, vol. 8, pp. 126504–126510, 2020.

[28] W. X. Jiang, Q. Cheng, and T. J. Cui, "Generation of high-directivity beams by using metasurfaces," in *Proc. Prog. Electromagn. Res. Symp. (PIERS)*, Aug. 2016, p. 3148.

[29] M. Qing Qi, W. X. Tang, and T. J. Cui, "A broadband Bessel beam launcher using metamaterial lens," *Sci. Rep.*, vol. 5, no. 1, p. 11732, Dec. 2015.

[30] A. Ciattoni and C. Palma, "Nondiffracting beams in uniaxial media propagating orthogonally to the optical axis," *Opt. Commun.*, vol. 224, nos. 4–6, pp. 175–183, Sep. 2003.

[31] J. Durnin, "Exact solutions for nondiffracting beams. I. The scalar theory," *J. Opt. Soc. Amer. A, Opt. Image Sci.*, vol. 4, no. 4, pp. 651–654, 1987.

[32] S. Chavez-cerda, "A new approach to Bessel beams," *Optica Acta Int. J. Opt.*, vol. 46, no. 6, pp. 923–930, 1999.

[33] J. D. Rosny and M. Fink, "Overcoming the diffraction limit in wave physics using a time-reversal mirror and a novel acoustic sink," *Phys. Rev. Lett.*, vol. 89, no. 12, Aug. 2002, Art. no. 124301.

[34] G. Lerosey, J. D. Rosny, A. Tourin, A. Derode, G. Montaldo, and M. Fink, "Time reversal of electromagnetic waves," *Phys. Rev. Lett.*, vol. 92, no. 19, May 2004, Art. no. 193904.

[35] J. D. Rosny, G. Lerosey, and M. Fink, "Theory of electromagnetic time-reversal mirrors," *IEEE Trans. Antennas Propag.*, vol. 58, no. 10, pp. 3139–3149, Oct. 2010.

[36] G. Lerosey, J. D. Rosny, A. Tourin, A. Derode, and M. Fink, "Time reversal of wideband microwaves," *Appl. Phys. Lett.*, vol. 88, no. 15, 2006, Art. no. 154101.

[37] X. Zhao, S. Xiao, and Y. Sun, "A fully electronic time reversal mirror system based on temporal imaging," *IEEE Access*, vol. 7, pp. 16711–16717, 2019.

QING-SONG JIA was born in Sichuan, China, in 1997. He received the B.E. degree in electronic information science and technology from the University of Electronic Science and Technology of China, in 2019, where he is currently pursuing the M.E. degree in electromagnetic field and microwave technology with the School of Physics. His current research interests include metasurface, antenna arrays, and the application of radio OAM vortex wave.

SHUAI DING received the Ph.D. degree in radio physics from the University of Electronic Science and Technology of China (UESTC), Chengdu, in 2013. From 2013 to 2014, he was a Postdoctoral Associate with the École Polytechnique de Montréal, Montréal, QC, Canada. In 2015, he joined UESTC, where he is currently an Associate Professor. He has authored or coauthored over 80 publications in refereed journals and international conferences/symposia. His current research interests include time-reversed electromagnetics and its applications to communication and energy transmission, phased array, analog signal processing, and microwave circuits. He has served as a TPC Member for various conferences and a reviewer for several peer-reviewed periodicals and international conferences/symposia.

HUI-BING DONG was born in Sichuan, China, in 1995. He received the B.E. degree in electronic information science and technology from the University of Electronic Science and Technology of China, in 2017, and the M.E. degree in electromagnetic field and microwave technology with the School of Physics, University of Electronic Science and Technology of China, in 2020. His current research interests include the design of microwave and millimeter-wave circuits.

XU HAN was born in Sichuan, China, in 1995. He received the B.E. degree in electronic information science and technology from the University of Electronic Science and Technology of China, in 2018, where he is currently pursuing the Ph.D. degree in electromagnetic field and microwave technology with the School of Physics. His current research interests include metasurface, antenna arrays, and phase array.

ZHAO-JUN ZHU was born in Sichuan, China, in 1978. He received the B.S. degree and the Ph.D. degree in physical electronics from the University of Electronic Science and Technology of China (UESTC), Chengdu, in 2002 and 2007, respectively. Since 2012, he has been an Associate Professor with UESTC. His research interests include the design of microwave and millimeter-wave circuits.

BING-ZHONG WANG (Senior Member, IEEE) received the Ph.D. degree in electronic engineering from the University of Electronic Science and Technology of China (UESTC), Chengdu, in 1988. He joined UESTC, in 1984, where he is currently a Professor. He has been a Visiting Scholar with the University of Wisconsin–Milwaukee, Milwaukee, WI, USA, a Research Fellow with the City University of Hong Kong, Hong Kong, and a Visiting Professor with the Electromagnetic Communication Laboratory, Pennsylvania State University, University Park, PA, USA. His current research interests include computational electromagnetics, antenna theory and techniques, and time-reversed electromagnetics.

YONG MAO HUANG (Member, IEEE) received the B.S. degree in communication engineering and the Ph.D. degree in communication and information systems from the University of Electronic Science and Technology of China (UESTC), Chengdu, China, in 2010 and 2017, respectively.

From 2014 to 2015, he was with the Department of Electrical Engineering, University of South Carolina, Columbia, SC, USA. In 2018, he joined the School of Electrical and Electronic Information, Xihua University, where he is currently an Associate Professor. He has authored and coauthored nearly 60 refereed papers. He serves as a Reviewer for various IEEE/IET/Wiley/Elsevier/ACES periodicals and journals. His research interests include RF/microwave/millimeter-wave circuits and systems for wireless communication, radar and sensing applications, substrate integrated circuits, and reconfigurable components and antennas. He is a member of the ACES and the Chinese Institute of Electronics (CIE). He has served as the Co-Organizer/Co-Chair for Special Session of the 2020 IEEE MTT-S International Wireless Symposium, the Technical Program Committee Member for 2018/2020 IEEE MTT-S International Conference on Microwaves for Intelligent Mobility, and several other international conferences/symposia, and on the Editorial Board of the *Journal of Electrical and Electronic Engineering*.

MAURIZIO BOZZI (Fellow, IEEE) received the Ph.D. degree in electronics and computer science from the University of Pavia, Pavia, Italy, in 2000.

In 2002, he joined the Department of Electronics, University of Pavia, where he is currently a Full Professor of Electromagnetic Fields. He held research positions with various universities worldwide, including the Technische Universität Darmstadt, Germany; Universitat de Valencia, Spain; and the École Polytechnique de Montréal, Canada. He was also a Guest Professor (2015–2017) at Tianjin University, China, and a Visiting Professor (2017–2018) at the Gdansk University of Technology, Poland. He has authored/coauthored more than 140 journal papers and 330 conference papers. He has co-edited the book *Periodic Structures* (Research Signpost, 2006) and has also coauthored the book *Microstrip Lines and Slotlines* (Artech House, 2013). His main research interests concern the computational electromagnetics, the substrate integrated waveguide technology, and the use of novel materials and fabrication technologies for microwave circuits.

Prof. Bozzi is an Elected Member of the Administrative Committee of the IEEE Microwave Theory and Techniques Society (MTT-S) from 2017 to 2022, and the current MTT-S Treasurer. He received several awards, including the 2015 Premium Award for Best Paper in IET Microwaves, Antennas & Propagation, the 2014 Premium Award for the Best Paper in Electronics Letters, the Best Student Paper Award at the 2016 IEEE Topical Conference on Wireless Sensors and Sensor Networks (WiSNet2016), the Best Paper Award at the 15th Mediterranean Microwave Symposium (MMS2015), the Best Student Award at the 4th European Conference on Antennas and Propagation (EuCAP 2010), the Best Young Scientist Paper Award of the XXVII General Assembly of URSI in 2002, and the MECSA Prize of the Italian Conference on Electromagnetics (XIII RiNEm), in 2000. He was the Chair of the Meetings and Symposia Committee of MTT-S AdCom from 2018 to 2019, the Secretary of the IEEE MTT-S in 2016, and a member of the General Assembly (GA) of the European Microwave Association (EuMA) from 2014 to 2016. He was the General Chair of the IEEE MTT-S International Microwave Workshop Series-Advanced Materials and Processes (IMWS-AMP 2017), in Pavia, Italy, in 2017, of the inaugural edition of the IEEE International Conference on Numerical Electromagnetic Modeling and Optimization (NEMO2014), in Pavia, Italy, in 2014, and of the IEEE MTT-S International Microwave Workshop Series on Millimeter Wave Integration Technologies, in Sitges, Spain, in 2011. He is a Track Editor of the IEEE TRANSACTIONS ON MICROWAVE THEORY AND TECHNIQUES. He was an Associate Editor of the IEEE MICROWAVE AND WIRELESS COMPONENTS LETTERS, *IET Electronics Letters*, and *IET Microwaves, Antennas and Propagation*. He was the Guest Editor of special issues in the IEEE TRANSACTIONS ON MICROWAVE THEORY AND TECHNIQUES, the *IEEE Microwave Magazine*, and the *IET Microwaves, Antennas and Propagation*.

. . .